Supporting Information for:

Separation of Bio-Based Glucaric Acid via Antisolvent Crystallization and Azeotropic Drying

Hoon Choi[1], Nathan E. Soland[1,a], Bonnie L. Buss[1], Nora C. Honeycutt[1,b], Emily G. Tomashek[1,c], Stefan J. Haugen[1], Kelsey J. Ramirez[1], Joel Miscall[1], Eric C.D. Tan[1], Tyler N. Smith[2], Patrick O. Saboe[1], and Eric M. Karp[1,*]

1. Renewable Resources and Enabling Sciences Center, National Renewable Energy Laboratory, Golden Colorado 80401
2. Kalion Inc., 92 Elm St., Milton, MA 02186

* *Corresponding author:* eric.karp@nrel.gov
a. Current address: Department of Chemistry, University of California, Berkeley, CA 94720
b. Current address: Humm Kombucha, 20720 NE Brinson Blvd., Bend, OR 97701
c. Current address: LanzaTech, 8045 Lamon Ave., Suite 400, Skokie, IL 60077

Table of Contents

S1. Glucaric Acid (GA) Equilibration Calculation

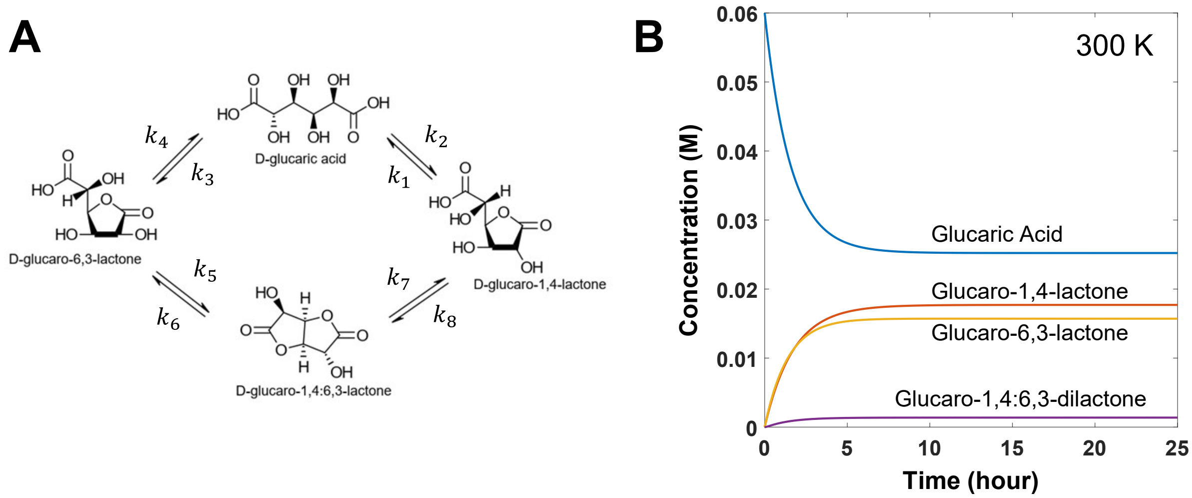

Figure S1: (A) Equilibrium of glucaric acid (GA) and lactones, (B) Simulation of GA equilibration at 300K based on rate constants given in Table S1.

Figure S1A shows the equilibration of glucaric acid (GA) and lactones with reaction coefficients. Each reaction coefficient was defined in Table S1. Figure S1B was obtained by calculating the following algebraic equations simultaneously.

$$\frac{dC_{GA}}{dt} =- (k_2 + k_3)C_{GA} + k_1 C_{1,4L} + k_4 C_{6,3L} \#(S1)$$

$$\frac{dC_{1,4L}}{dt} = k_2 C_{GA} - (k_1 + k_8)C_{1,4L} + k_7 C_{DL} \ \#(S2)$$

$$\frac{dC_{6,3L}}{dt} = k_3 C_{GA} - (k_4 + k_5)C_{6,3L} + k_6 C_{DL} \#(S3)$$

$$\frac{dC_{DL}}{dt} = k_8 C_{1,4L} - (k_6 + k_7)C_{DL} + k_5 C_{6,3L} \#(S4)$$

where 1,4L denotes 1,4-lactone; 6,3L denotes 6,3-lactone; DL denotes 1,4:6,3-dilactone. The value of each rate constant was obtained from the literature and listed in Table S1.[1]

Table S1: Rate constants for the equilibration of glucaric acid and lactones at 300K[1]

Rate constant	Reaction	Values (s^{-1})
k_1	1,4-lactone → GA	7.04×10^{-5}
k_2	GA → 1,4-lactone	4.84×10^{-5}
k_3	GA → 6,3-lactone	5.52×10^{-5}
k_4	6,3-lactone → GA	8.70×10^{-5}
k_5	6,3-lactone → 1,4:6,3-dilactone	1.74×10^{-4}
k_6	1,4:6,3-dilactone → 6,3-lactone	1.97×10^{-3}
k_7	6,3-lactone → 1,4:6,3-dilactone	6.64×10^{-4}

k_8	1,4:6,3-dilactone → 6,3-lactone	5.01×10^{-5}

S2. Solubility Measurements and Recovery of GA and Potassium Glucarate (KGA)

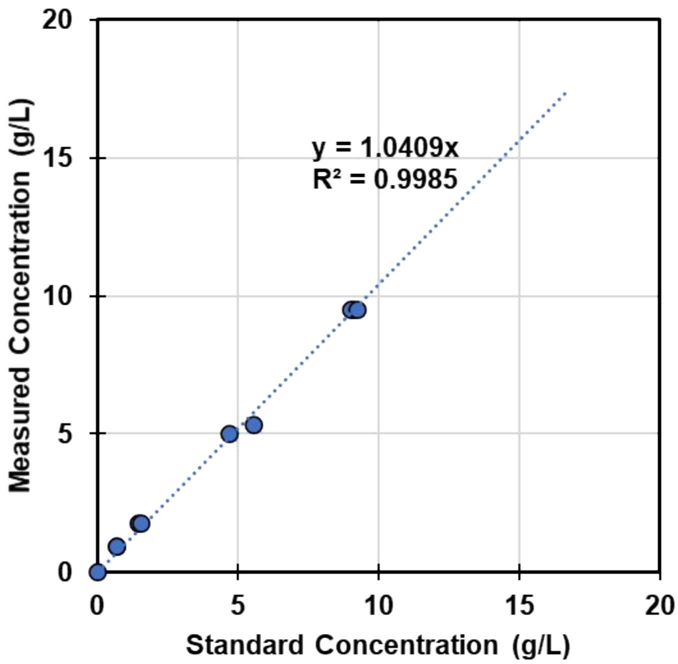

Figure S2: TGA calibration curve for GA solutions

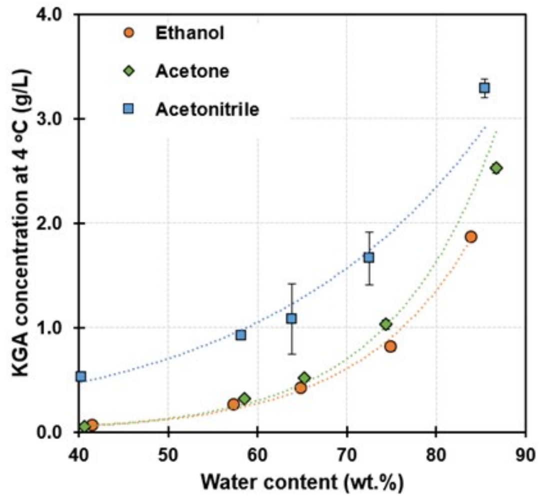

Figure S3: Solubility of potassium glucarate (KGA) in a solution of acetonitrile, acetone, or ethanol with varied water content at 4 ^{o}C

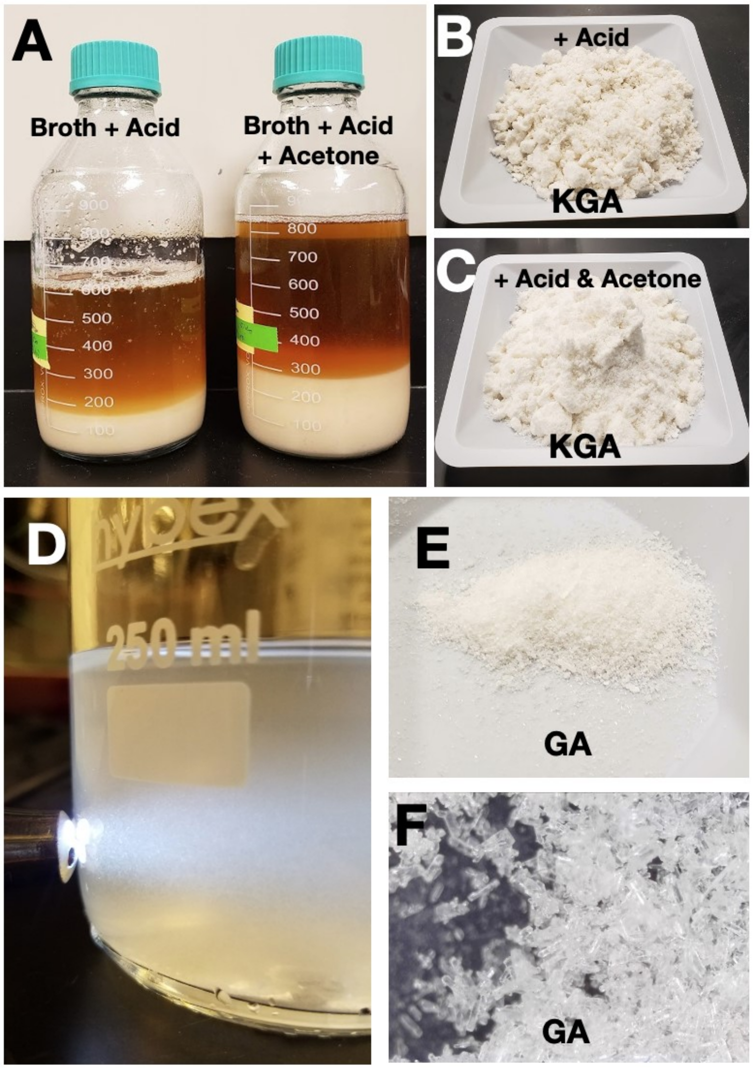

Figure S4: (A) Precipitation of KGA from the broth using acid addition (left) and acid and acetone addition method (right), (B) recovered KGA obtained from acid addition, (C) recovered KGA from acid and acetone addition method, (D) GA crystal seed formation after volume concentrated ten times via azeotropic drying, (E) recovered GA via antisolvent crystallization method, (F) Optical microscopy image of GA (x200 magnification)

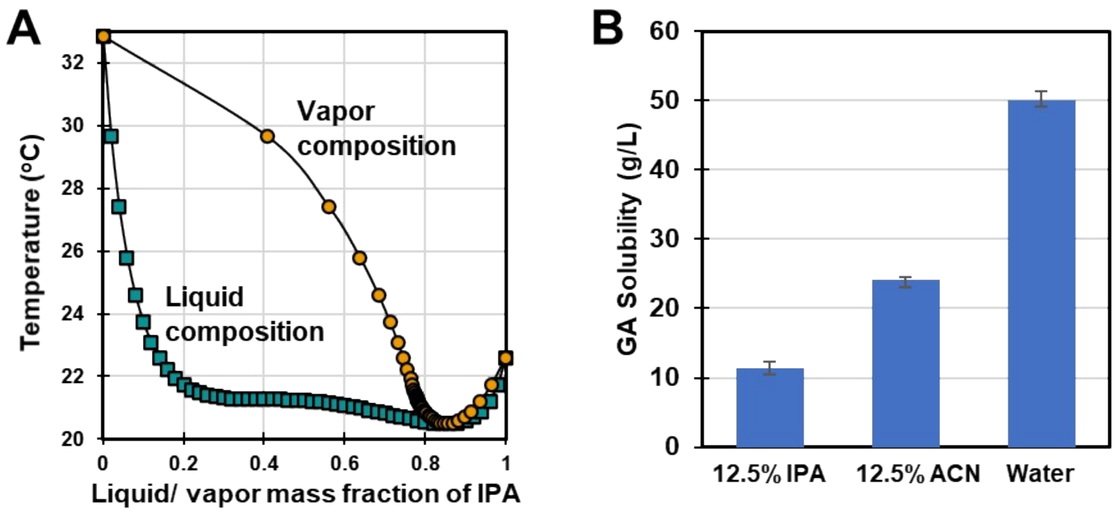

Figure S5: (A) Simulated Water-IPA phase diagram using an NRTL model at 50 mbar. The azeotrope formed when the W_{IPA} is 0.875. (B) Comparison of the antisolvent effect of isopropanol and acetonitrile on the GA solubility at 4 °C.

S3. Characterization of KGA and GA Products

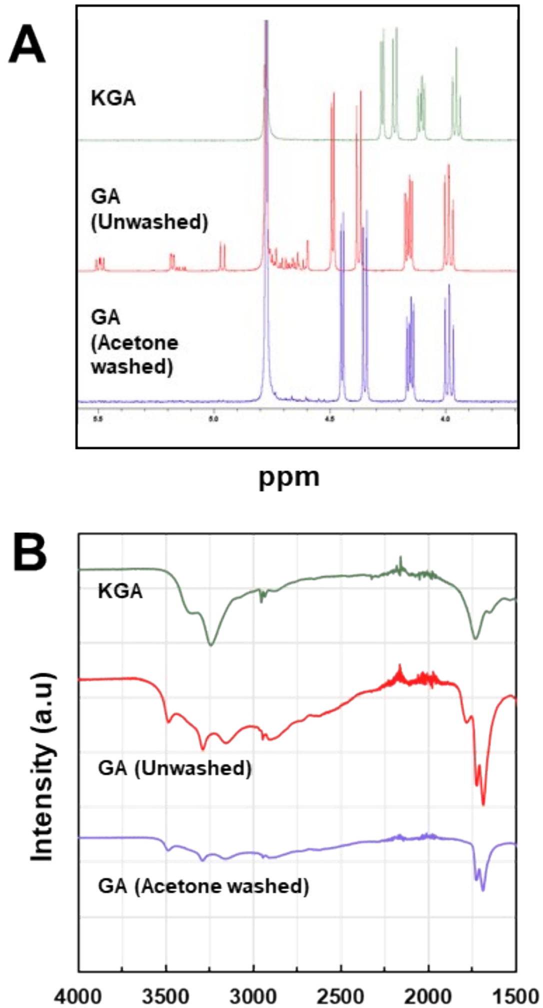

Figure S6: (A) ^{1}H-NMR and (B) FTIR spectra of the recovered products: KGA, unwashed GA, GA after an acetone wash.

In Figure S6B the strong peaks at 1683 and 1725 cm^{-1} in GA can be attributed to the two carboxylic acids C=O stretches. KGA contains these peaks as well, though with diminished intensity and the 1683 cm^{-1} peak shifted to 1640 cm^{-1} due to substitution of an acidic H^+ with K^+.[2,3] Strong peaks at 3480, 3293, 3172 cm^{-1} and the broad absorption between 3000-3500 cm^{-1} correspond to the O-H groups of the backbone and acids, and the medium stretching peaks around 2950 cm^{-1} can be attributed to the alkane C-H bonds.

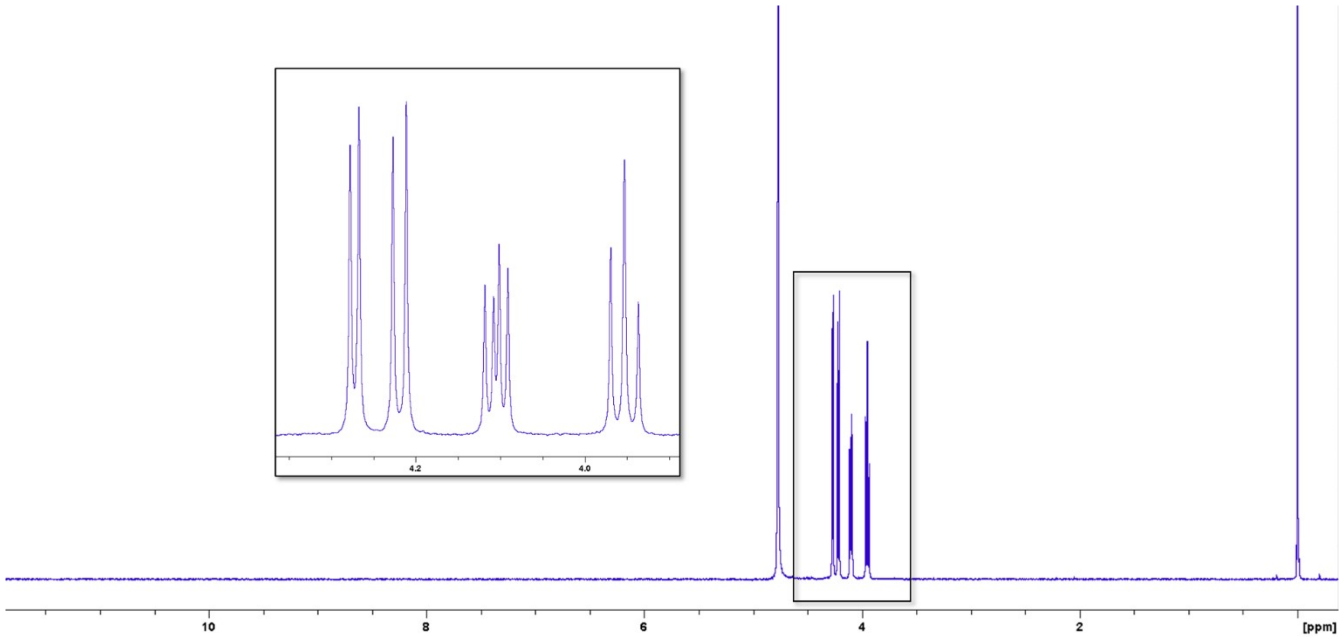

Figure S6-2: ^{1}H NMR spectrum for KGA ^{1}H NMR (300 MHz, D_2O) δ 4.27 (d, J = 3.1 Hz, 1H), 4.22 (d, J = 4.7 Hz, 1H), 4.170(dd, J = 3.1, 5.7 Hz, 1H), 3.95 (t, J = 4.9 Hz, 1H).

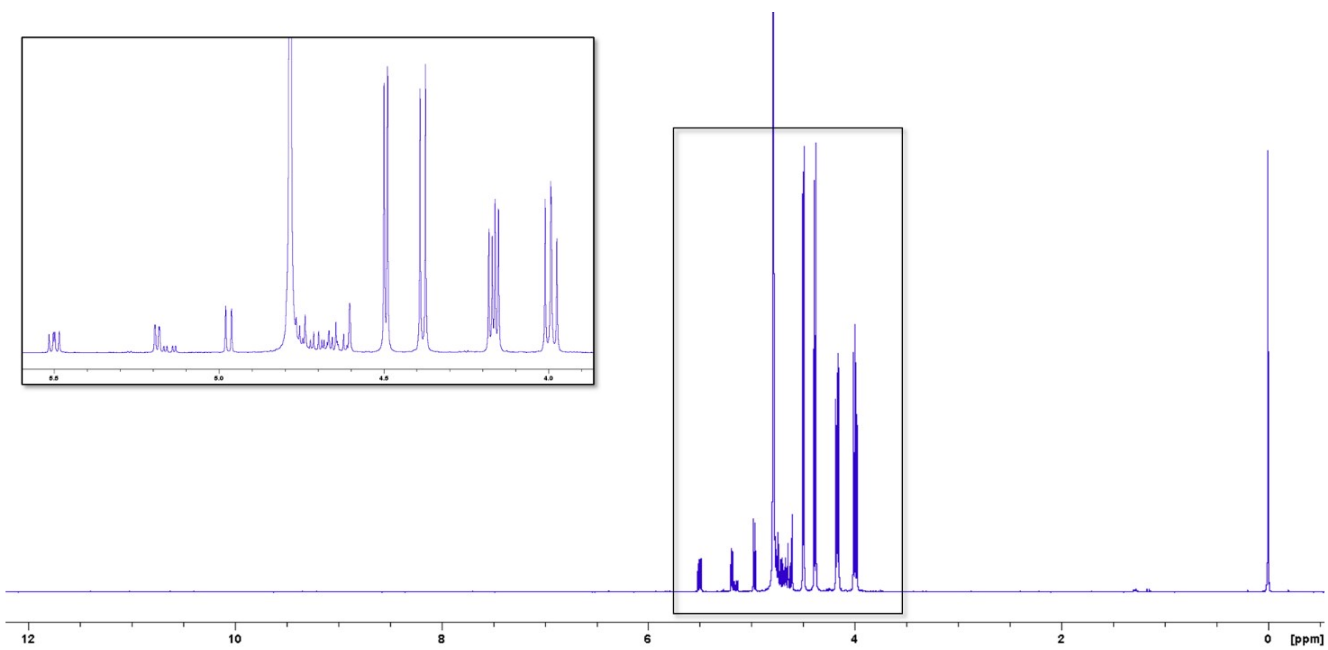

Figure S6-3: ^{1}H NMR spectrum for unwashed GA showing the presence of lactone impurities. The following multiplet report is for the GA molecule only: ^{1}H NMR (300 MHz, D_2O) δ 4.49 (d, J = 3.1 Hz, 1H), 4.38 (d, J = 5.0 Hz, 1H), 4.17 (dd, J = 3.1, 5.7 Hz, 1H), 3.99 (q, J = 3.6 Hz, 1H).

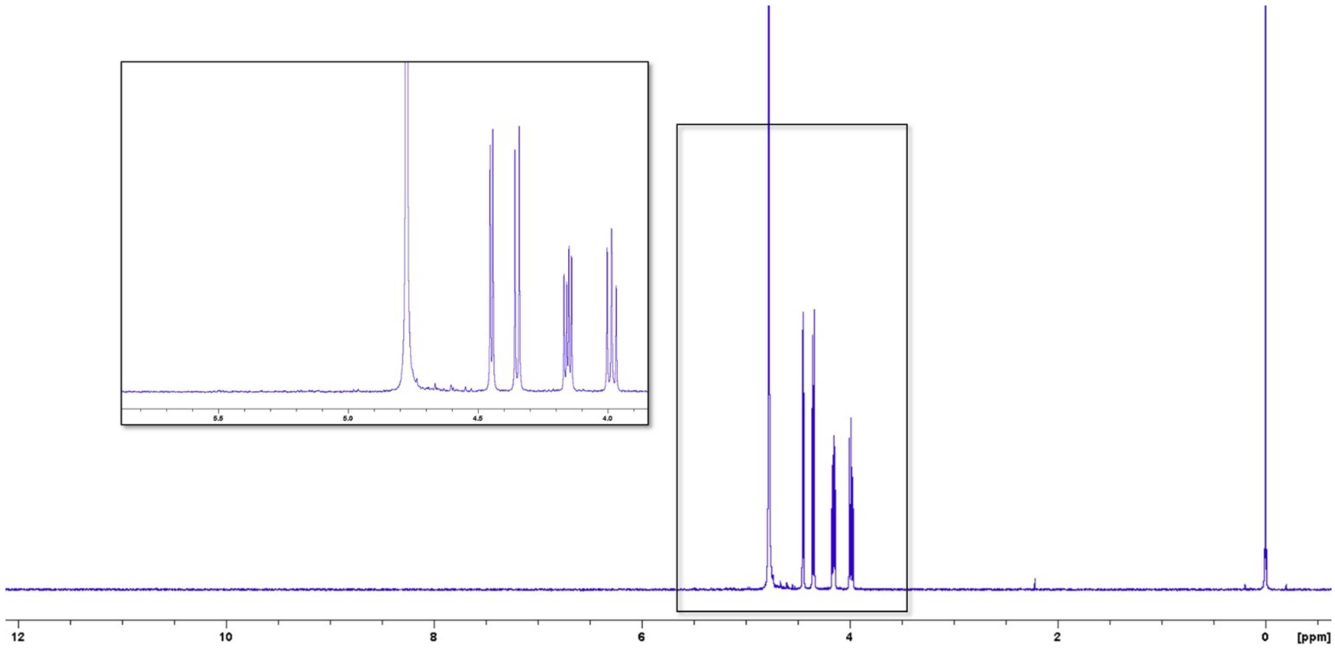

Figure S6-4: ^1H NMR spectrum for washed GA. ^1H NMR (300 MHz, D_2O) δ 4.45 (d, *J* = 3.1 Hz, 1H), 4.35 (d, *J* = 4.9 Hz, 1H), 4.17 (q, *J* = 2.9 Hz, 1H), 3.98 (q, *J* = 3.5 Hz, 1H).

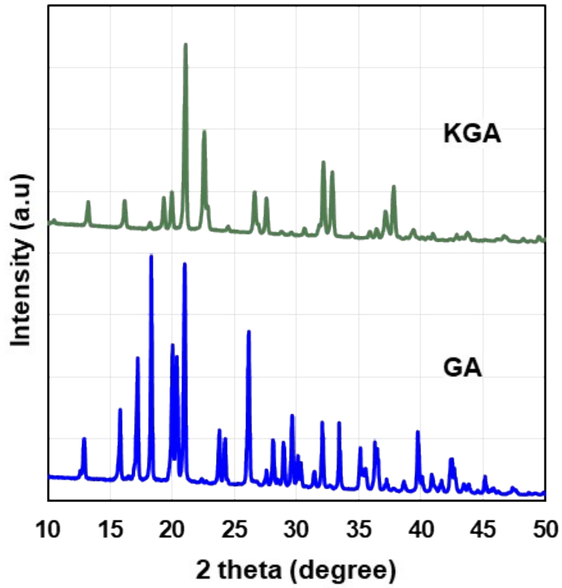

Figure S7: XRD pattern of KGA (upper) and GA (lower)

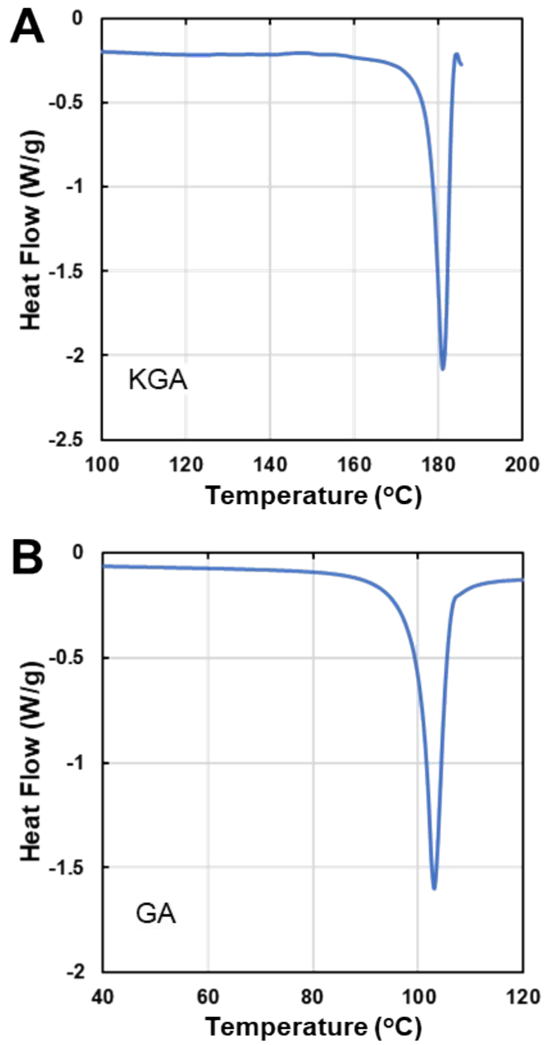

Figure S8: DSC curve of (A) KGA and (B) GA

S4. Aspen Plus Models of KGA and GA Downstream Processes

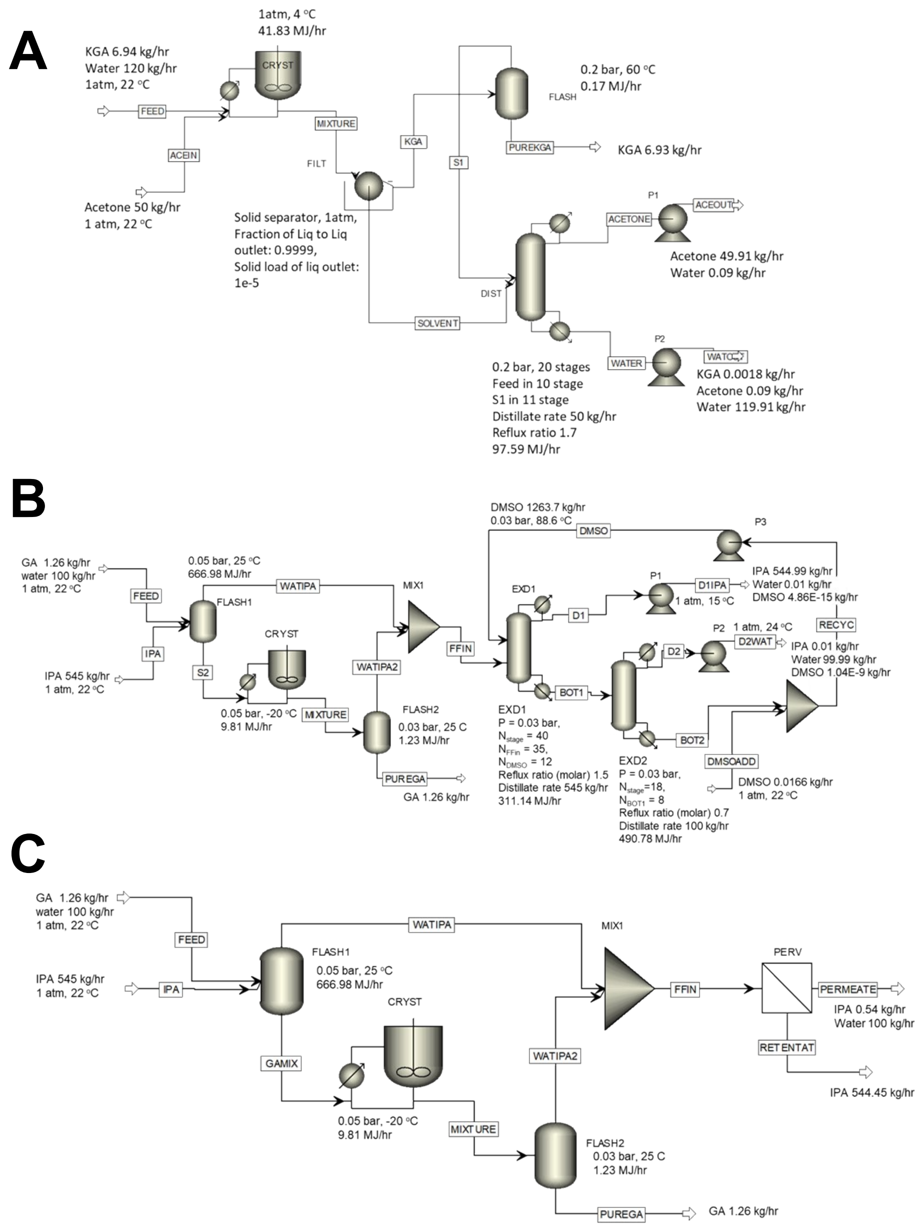

Figure S9: Aspen Plus models for the crystallization and solvent recovery of (A) KGA, (B) GA with the extractive distillation process, and (C) GA with the pervaporation process

Aspen Plus models for KGA and GA recovery systems were built based on a UNIFAC model (Figure S9). Crystallization property setup was determined based on either literature or experimental data. Crystallization reactions for KGA and GA were set as $KGA\ (l) \rightarrow KGA(s)$ and $GA(l) \rightarrow GA(s)$, respectively. Solubility data was obtained from experimental results presented in Figure 6. Solid molar volume (V_m) was calculated based on the unit cell parameters obtained from the literature XRD data as shown below.[2,4]

$$V_m = \frac{N_A}{Z} V_{cell} = \frac{N_A}{2} abc|\sin \beta| \quad for\ monoclinic\ structure(\ Z = 2)\ \#(S5)$$

where N_A is Avogadro's number, V_{cell} is the unit cell volume, Z is the number of formula units per unit cell; $a, b, c,$ and β are the unit cell dimensions. Eq. (S5) provides V_m for KGA and GA as 272.19 cm^3/mol and 127.03 cm^3/mol, respectively. Solid heat capacity (C_p) correlation parameters in Eq. S6 were obtained by fitting a $C_p(T)$ curve measured from DSC curves in Figure S8 and presented in Table S2.

$$C_p^s = C_1 + C_2 T + C_3 T^2 + \frac{C_4}{T} + \frac{C_5}{T^2} + \frac{C_6}{\sqrt{T}} \quad \#(S6)$$

Table S2: Input parameters for calculating $C_p(T)$ in Aspen Plus

	C_1	C_2	C_3	C_4	C_5	C_6
KGA	0.1669	0.01668	-4.3E-05	0	0	0
GA	0.2952	0.000385	2.94E-05	0	0	0

Figure S9B showed a solvent and product recovery model for GA with an extractive distillation process as illustrated in Figure 4B. Please note that a solvent recovery step for GA was calculated using an NRTL model. For the extractive distillation, dimethylsulfoxide (DMSO) was used as an entrainer. The binary parameters for calculating activity coefficients were obtained from Arifin and Chien's data (Table S3).[5] Also, the temperature and pressure of two flash distillations were determined based on the sensitivity analysis, which was set to separate the GA from solvent streams with >99.9% yield.

In Figure S9C, a solvent recovery process was modeled with a pervaporation (PV) process by assuming the membrane can allow largely water to diffuse through the membrane pore and undergo phase change under the adiabatic pervaporation mode at low pressure. The recovered water/IPA mixture went through the PV process such that water is evaporated and then condensed in the permeate stream (>99% purity) while IPA was recovered at the retentate stream with >99.9 % yield and >99.0 % purity.

Table S3: Binary parameters used in NRTL model

$comp, i$	IPA	IPA	H2O
$comp, j$	H2O	DMSO	DMSO
a_{ii}	0	0	-1.2449
a_{ji}	0	0	1.7524
b_{ij}	185.4	115.2787	586.801
b_{ji}	777.3	-25.0123	-1130.22
c_{ij}	0.5	0.3	0.3

Table S4: Mass flow rate, temperature, and pressure of streams in **Figure S9A**

Streams	FEED	ACEIN	MIXTURE	KGA	SOLVENT	S1	PUREKGA	ACEOUT	WATOUT
Total Mass Flows (kg/hr)	126.94	50.00	176.94	6.95	169.99	0.02	6.94	50.00	120.00
ACN (kg/hr)	0.00	0.00	0.00	0.00	0.00	0.00	0.00	0.00	0.00
KGA (kg/hr)	6.94	0.00	0.00	0.00	0.00	0.00	0.00	0.00	0.00
WATER (kg/hr)	120.00	0.00	120.00	0.01	119.99	0.01	0.00	0.09	119.91
KGA (S) (kg/hr)	0.00	0.00	6.94	6.94	0.00	0.00	6.94	0.00	0.00
ACETONE (kg/hr)	0.00	50.00	50.00	0.00	50.00	0.00	0.00	49.91	0.09
Temperature (°C)	22.00	22.00	4.00	4.00	4.00	60.00	60.00	15.39	59.77
Pressure (bar)	1.013	1.013	1.013	1.013	1.013	0.200	0.200	1.013	1.013

Table S5: Mass flow rate, temperature, and pressure of streams in **Figure S9B**

Streams	FEED	IPA	WATIPA	S2	MIXTURE	WATIPA2	PUREGA	FFIN
Mass Flows (kg/hr)	101.26	545.00	644.31	1.95	1.95	0.69	1.26	645.00
GA (kg/hr)	1.26	0.00	0.00	1.26	0.00	0.00	0.00	0.00
GA (S) (kg/hr)	0.00	0.00	0.00	0.00	1.26	0.00	1.26	0.00
WATER (kg/hr)	100.00	0.00	99.65	0.35	0.35	0.35	0.00	100.00
PROPANOL (kg/hr)	0.00	545.00	544.66	0.34	0.34	0.34	0.00	545.00
DMSO (kg/hr)	0.00	0.00	0.00	0.00	0.00	0.00	0.00	0.00
Temperature (°C)	22.00	14.80	25.00	25.00	-20.00	25.00	25.00	25.00
Pressure (bar)	1.01	0.03	0.05	0.05	0.05	0.03	0.03	0.05

Streams in the extractive distillation process

Streams	D1	D1IPA	BOT1	D2	D2WAT	BOT2	DMSO ADD	RECYC	DMSO
Mass Flows (kg/hr)	545.00	545.00	1395.80	100.00	100.00	1295.80	0.02	1295.82	1295.82
GA (kg/hr)	0.00	0.00	0.00	0.00	0.00	0.00	0.00	0.00	0.00
GA (S) (kg/hr)	0.00	0.00	0.00	0.00	0.00	0.00	0.00	0.00	0.00
WATER (kg/hr)	0.01	0.01	100.02	99.99	99.99	0.04	0.00	0.04	0.04
PROPANOL (kg/hr)	544.99	544.99	0.01	0.01	0.01	0.00	0.00	0.00	0.00
DMSO (kg/hr)	0.00	0.00	1295.76	0.00	0.00	1295.76	0.02	1295.78	1295.78
Temperature (°C)	14.84	14.88	62.63	24.05	24.15	88.68	22.00	88.69	88.75
Pressure (bar)	0.03	0.03	0.03	0.03	1.01	0.03	1.01	0.03	0.05

Table **S6:** Mass flow rate, temperature, and pressure of streams in **Figure S9C**

Streams	FEED	IPA	GAMIX	MIXTURE	PUREGA	WATIPA	WATIPA2	FFIN	PERMEATE	RETENTAT
Mass Flows (kg/hr)	101.26	545	1.95	1.95	1.26	644.31	0.69	645	100.54	544.46
GA (kg/hr)	1.26	0	1.26	0	0	0	0	0	0	0
GA (S) (kg/hr)	0	0	0	1.26	1.26	0	0	0	0	0
WATER (kg/hr)	100	0	0.35	0.35	0	99.65	0.35	100	100	0
PROPANOL (kg/hr)	0	545	0.34	0.34	0	544.66	0.34	545	0.54	544.46
Temperature (°C)	22	22	25	-20	25	25	25	25	76.16	14.84
Pressure (bar)	1.01	1.01	0.05	0.05	0.03	0.05	0.03	0.05	0.41	1.3

S5. Modeling and Simulation for Designing a Cation Exchange Process

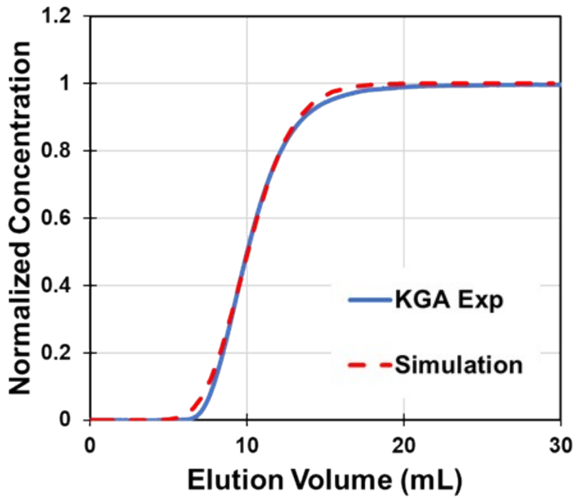

Figure S10. KGA (0.06 M) breakthrough curve compared with a rate model simulation

Figure S10 shows the experimental data of the KGA breakthrough curve and the simulation data. The simulation was conducted using Aspen Chromatography V10 simulator based on the experimental conditions. The input parameters including selectivity and mass transfer coefficients were referred from the literature and vendor information. For instance, the sorbent selectivity (α) was determined as 2.54 from the manufacturer's specification.[6] The axial dispersion coefficient, Brownian diffusivity coefficient, and intraparticle diffusion coefficient were referred from the literature values.[7] The simulated curve agreed well with experimental data in Figure S10. The input parameters are summarized in Table S7. With respect to the difference of mass transfer zone in elution volume, the simulation showed a 4.7% error compared to the experimental data.

As an example, we designed a CEX process at a preparative scale with the column size of 10 cm inner diameter and 60 cm length and the same intrinsic parameters as presented in Table S7. Based on Equation 2 and 3, the maximum loading volume ($V_{f,max}$) of 0.1 M KGA for a single column is 85.37 L under the flowrate of 250 ml/min and 1% breakthrough cut. For designing a simple carousel process that switches all ports at the same time as illustrated in Figure 6, we can use the calculated $V_{f,max}$ and the flowrate for the loading step (step 1) such that the port switching time is set as 341 min, and the flowrate for other steps can be determined (usually faster than the loading flowrate) to elute all species out before the switching time.

Table S7. Simulation input parameters used in Aspen Chromatography V10. Note that default values are used for other parameters.

System Parameters and Operating conditions

Column length, L_c (cm)	Column diameter (cm)	Resin particle radius, R_p (μm)	Bed porosity, ε_b	Intraparticle porosity, ε_p
10	1.6	325	0.34	0.27
Mobile phase density (kg/m^3)	Mobile phase viscosity (cP)	Feed concentration (mequiv./ml)	Flowrate (ml/min)	Size exlculsion factor
996	0.89	0.06	2.5	1

Isotherm and mass transfer models and parameters

Isotherm model		Kinetic model	Film mass transfer	Axial dispersion
Mass action equilibrium		Particle MB (Rate model)	Wilson and Geankoplis correlation[8]	Constant dispersion
Sorbent selectivity,	Column capacity (mequiv./ml)	Intraparticle diffusion coefficient, D_p (cm^2/min)	Brownian diffusivity in the liquid phase, D_b (cm^2/min)	Axial dispersion coefficient, E_b (cm^2/min)
2.54	2	1.176×10^{-3}	1.176×10^{-3}	1.069×10^{-2}

Numerical methods and parameters

Integration method	PDE method	Axial elements	Collocation points in particle phase	Tolerance (absolute)	Tolerance (relative)	Time step size
implicit Euler	QDS	100 nodes	4 nodes	0.0005	0.0005	Variable (0.1 ~ 0.5)

References

1 J. M. Brown, M. Manley-Harris, R. J. Field and D. E. Kiely, J. Carbohydr. Chem., 2007, 26, 455–467.

2 T. T. Denton, K. I. Hardcastle, M. K. Dowd and D. E. Kiely, Carbohydr. Res., 2011, 346, 2551–2557.

3 R. D. Armstrong, B. M. Kariuki, D. W. Knight and G. J. Hutchings, European J. Org. Chem., 2017, 2017, 6811–6814.

4 T. Taga, Y. Kuroda and K. Osaki, Bull. Chem. Soc. Jpn., 1977, 50, 3079–3083.

5 S. Arifin and I. L. Chien, Ind. Eng. Chem. Res., 2008, 47, 790–803.

6 Lenntech, *https://www.lenntech.com/Data-sheets/Dowex-Ion-Exchange-Resins-Using-Selectivity-Coefficients-L.pdf (Lastly accessed on 11/22/2021).*

7 M. V. J. Ernest, R. D. Whitley, Z. Ma and N.-H. L. Wang, Ind. Eng. Chem. Res., 1997, 36, 212–226.

8 E. J. Wilson and C. J. Geankoplis, Ind. Eng. Chem. Fundam., 1966, 5, 9–14.